The Journal of Nutrition
Nutritional Immunology

Lactobacillus reuteri 100-23 Transiently Activates Intestinal Epithelial Cells of Mice That Have a Complex Microbiota during Early Stages of Colonization[1–3]

Micha Hoffmann,[4,7] Eva Rath,[4,7] Gabriele Hölzlwimmer,[5] Leticia Quintanilla-Martinez,[5] Diane Loach,[6] Gerald Tannock,[6] and Dirk Haller[4]*

[4]Chair for Biofunctionality, Nutrition and Food Research Center, Technische Universität München, 85350 Freising-Weihenstephan, Germany; [5]Helmholtz Center Munich, Institute of Pathology, 85764 Neuherberg, Germany; and [6]Department of Microbiology, University of Otago, PO Box 56 Dunedin, New Zealand

Abstract

Monoassociations of germ-free animals with colitogenic and probiotic bacterial strains trigger intestinal epithelial cell (IEC) activation and host-derived feedback mechanisms. To characterize the impact of a single nonpathogenic bacterial strain on the intestinal epithelium in the presence of an established microbiota, we inoculated reconstituted *Lacotobacillus*-free (RLF) mice at 8 wk of age with *Lactobacillus reuteri* 100-23. Primary IEC from the small intestine of *L. reuteri*-inoculated and control RLF mice were isolated 2, 6, and 21 d after inoculation followed by gene expression analysis (real-time PCR; Affymetrix microarrays) as well as 2-dimensional-gel electrophoreses (2D SDS-PAGE) and peptide mass fingerprinting via matrix-assisted laser desorption/ionization time of flight MS. At d 6, gene expression of proinflammatory cytokines and chemokines including interleukin (IL)-1α, IL-6, interferon-γ-inducible protein 10, and macrophage inflammatory protein 2 was transiently induced, whereas gene expression levels of regulatory proteins A20 and Toll-interacting protein decreased. In addition, 8 target proteins with changes in the steady-state protein expression levels were identified at d 2 and 6 of *L. reuteri* colonization. Consistent with the absence of histopathology, *L. reuteri*-induced activation of primary IEC returned to control levels by d 21 after inoculation of RLF mice. The capability of *L. reuteri* 100-23 to directly trigger epithelial cell activation was confirmed in small IEC cultures using the murine cell line Mode-K. These results clearly indicate that the intestinal epithelium is reactive toward environmental changes induced by the commensal bacterial strain *L. reuteri* even in the presence of an already-established microbiota. The induction of transient IEC activation may help to maintain mucosal homeostasis. J. Nutr. 138: 1684–1691, 2008.

Introduction

The mucosal surfaces and cavities of the gastrointestinal tract in mammals contain an extremely diverse and dense flora of microorganisms that are normally nonpathogenic to an immunocompetent host. Despite the abundance of bacterial molecules that can potentially activate bacterial molecular pattern receptors to trigger damaging innate immune responses and inflammation (1), it is a characteristic feature of the mucosal immune system in the normal host that protective immune responses against enteropathogenic organisms are allowed to proceed while responses to microorganisms of the indigenous microbiota are prevented. There is increasing evidence that a loss of this complex homeostasis in the genetic susceptible host may contribute to chronic activation of proinflammatory immune mechanisms and initiation and/or perpetuation of chronic intestinal inflammation such as inflammatory bowel diseases (IBD),[8] including ulcerative colitis and Crohn's disease (CD) (2).

Interestingly, there is accumulating evidence that intestinal epithelial cells (IEC) not only participate in nutrient uptake but also contribute to the initiation and regulation of innate and adaptive defense mechanisms (3). IEC directly interact with enteric luminal bacteria as well as with lamina propria dendritic cells, macrophages and lymphocytes, and intraepithelial lym-

[1] Supported by the German Academic Exchange Service.
[2] Author disclosures: M. Hoffmann, E. Rath, G. Hölzlwimmer, L. Quintanilla-Martinez, D. Loach, G. Tannock, and D. Haller, no conflicts of interest.
[3] Supplemental Tables 1–3 and Supplemental Figures 1 and 2 are available with the online posting of this paper at jn.nutrition.org.
[7] These authors contributed equally to the manuscript.
* To whom correspondence should be addressed. E-mail: haller@wzw.tum.de.

[8] Abbreviations used: CD, Crohn's Disease; 2D, 2-dimensional; ER, endoplasmic reticulum; grp, glucose-regulated protein; IBD, inflammatory bowl disease; IEC, intestinal epithelial cells; IEF, isoelectric focusing; I-FABP, intestinal fatty acid-binding protein; IL, interleukin; IP-10, interferon-γ-inducible protein 10; MALDI-TOF, matrix-assisted laser desorption/ionization time of flight; MIP-2, macrophage inflammatory protein 2; NF, nuclear factor; RLF, reconstituted *Lacotobacillus*-free; TLR, Toll-like receptor; TOLLIP, Toll-interacting protein.

Manuscript received 15 February 2008. Initial review completed 23 April 2008. Revision accepted 26 June 2008.

phocytes and are therefore considered to be a constitutive component of the mucosal immune system (3-5).

Although the impact of the endogenous luminal microbiota on the development and maturation of gut homeostasis including effects on epithelial cell functions has been illustrated by comparative studies of germ-free and conventionalized animals (6-8), little is known about the intestinal mucosal responses to the nonpathogenic intestinal microbiota in the normal host. It is unlikely that experimental outcomes from gnotobiotic studies are applicable to murine hosts that are colonized by a complex microbiota and have experienced a succession of quantitative and qualitative changes in microbiota composition during early life.

Because the aim of our study was to characterize the impact of a single nonpathogenic bacteria strain on the intestinal epithelium in the presence of an already-established microbiota, we used the unique animal model of reconstituted *Lacotobacillus*-free (RLF) mice. RLF mice were originally derived by antibiotic treatment followed by the stepwise addition of specific bacteria and a nonspecific mixture of microbes to the microbiota, resulting in an intestinal microbiota that is the functional equivalent of conventional mice but completely lacks lactobacilli (9). The descendants of these animals were maintained in isolators. Inoculating RLF mice with the commensal bacteria strain *Lactobacillus reuteri* 100-23 offers an excellent opportunity to investigate host-bacteria interactions in an already immune-maturated gut.

Methods

Animals and bacterial inoculation. RLF BALB/c mice (originally derived and obtained by Prof. Gerald W. Tannock, University of Otago, Dunedin, New Zealand) (9) were inoculated by mouth at 8 wk of age with a pure culture of *L. reuteri* 100-23 that was shown to colonize RLF mice after a single inoculation (10). The mice were maintained in isolators at the University of Otago and fed a standard rodent nonpurified diet (Diet 86, Sharpes' Stock Foods; composition shown in **Supplemental Table 1**) that had been sterilized by γ-irradiation. Colonization by *L. reuteri* 100-23 and absence of *lactobacilli* were confirmed, respectively, by culturing serial fecal samples and samples from the small (ileum, jejunum) and large intestine (cecum, colon) at necropsy. Inoculation of mice and culturing of samples was performed as previously described (11,12). Mice were killed by CO_2 anesthesia followed by cervical dislocation 2, 6, and 21 d after inoculation with *L. reuteri* 100-23. At each time point, RLF mice were used as controls. All animal experiments were conducted with approval of the University of Otago Animal Ethics Committee, approval number 104/02. Sections of the ileum were fixed in 10% neutral buffered formalin and embedded in paraffin. Histopathological analysis was performed at the Institute of Pathology (Helmholtz Center Munich, Munich-Neuherberg, Germany) as previously described (13). Briefly, 2 separate histological scores were assigned for epithelial damage (0-6) and infiltration with inflammatory cells (0-6) and added, resulting in a total scoring rage of 0-12.

Cell culture and bacterial infection. The murine IEC line Mode-K (passage 10-30) was grown in a humidified 5% CO_2 atmosphere at 37°C to confluency in 6-well tissue culture plates (Cell Star, Greiner bio-one) as previously described (14). Where indicated, the confluent epithelial cell monolayers were infected for various time points with *L. reuteri* 100-23 at a bacterium:epithelial cell ratio (multiplicity of infection) of 30 as previously described (14).

Isolation of primary mouse IEC. Primary IEC from the ileal and jejunal epithelium of control RLF mice and *L. reuteri* 100-23-colonized RLF mice were purified as previously described (14). Briefly, the ileal and jejunal tissue were cut into pieces and incubated at 37°C in DMEM containing 10% fetal calf serum and 1 mmol/L dithiothreitol for 30min. The remaining tissue was incubated in 30 mL PBS (1×) containing 1.5 mmol/L EDTA for an additional 10 min. The supernatants were filtered, centrifuged at 300 × *g*; 5 min, and the cell pellet was resuspended in DMEM containing 10% FCS. Finally, the primary IEC suspension was purified by centrifugation through a 20/40% discontinuous Percoll gradient at 600 × *g*; 30 min. Primary mouse IEC from ileum and jejunum were combined and collected in sample buffer for subsequent RNA isolation, Western blot, and proteome analysis.

Western blot analysis. Purified primary IEC or Mode-K cells were lysed in 1× Laemmli buffer and 50 μg of protein was subjected to electrophoresis on 15% [anti-CD3 and anti-intestinal fatty acid-binding protein (I-FABP) Western blots] or 10% SDS-PAGE gels. Anti-CD3 (Cell Signaling), anti-ERp57 [glucose-regulated protein (grp)-58; Stressgen], anti-CD19, anti-Integrin αX, anti-I-FABP (all from Santa Cruz Biotechnology), and anti-β-actin (ICN) were used to detect immunoreactive CD3, grp-58, CD19, Integrin αX, I-FABP, and β-actin, respectively, using an enhanced chemiluminescence light-detecting kit (Amersham).

RNA isolation and real-time RT-PCR. RNA from purified primary IEC and Mode-K cells was extracted using Trizol Reagent (Invitrogen Life Technologies) according to the manufacturer's instructions. Extracted RNA was dissolved in 20 μL water containing 0.1% diethylpyrocarbonate. The RNA concentration and purity (A_{260}:A_{280} ratio) was determined by spectrophotometric analysis (Nanodrop photometer). RT was performed from 1 μg total RNA. Real-time PCR was performed from 1 μL reverse-transcribed cDNA in glass capillaries using a Light CyclerTM system (Roche Diagnostics) as previously described (14). Primer sequences are given in **Supplemental Table 2**. The amplified product was detected by the presence of a SYBR green fluorescent signal. Melting curve analysis and gel electrophoresis was used to document the amplicon specificity. The crossing point of the log-linear portion of the amplification curve was determined. The relative induction of gene mRNA expression was calculated using the following equation: EΔcrossing point (control samples - treated samples) and normalized for the expression of 18S. All 5 samples from *L. reuteri* 100-23-colonized RLF mice were measured and blotted as fold of control RLF mice ($n = 5$) of the same time point. For the cell culture experiments, *L. reuteri* 100-23-treated Mode-K cells were measured and blotted as fold of untreated controls.

Affymetrix microarray. Expression profiling by Affymetrix microarray was performed with samples taken at d 6 after inoculation with *L. reuteri* 100-23. Three samples from single *L. reuteri* 100-23-colonized RLF mice were compared with 3 samples from single control RLF mice. RNA preparation, RT, labeling, and hybridization were conducted using the kits provided in the One-Cycle Target Labeling and Control Reagents package (Affymetrix) according to the Affymetrix Technical Manual. All samples were hybridized to the murine genome array NuGO_Mm1a 520177 (Affymetrix). The gene chips were washed and stained using a fluidics station and scanned with a GeneChip Scanner 3000 (all from Affymetrix). Data were analyzed using Affymetrix GCOS Manager and Genomatix ChipInspector.

The $\log_2$ fold change for each sample and probe set vs. each of the 3 control samples was calculated and the mean fold change of the *L. reuteri* group vs. the control group was determined. To test the significance of the difference in gene expression at the single probe level, a single-sided permutation *t* test analysis was performed. The probes were then mapped onto the relevant transcripts using Genomatix proprietary genome annotation. A transcript was considered as differentially expressed if at least 3 associated probes showed a mean absolute $\log_2$ fold change that was >0.5 (corresponds to a mean absolute fold change >1.41) and a *P*-value < 0.05. Bibliometric analysis for cocitation was performed using Bibliosphere Pathway Edition from Genomatix (Genomatix Software).

Sample preparation for 2-dimensional-PAGE and gel analysis. Protein from purified primary IEC from control RLF mice and *L. reuteri* 100-23-colonized RLF mice was isolated and subjected to isoelectric focusing (IEF) in the first dimension and SDS-PAGE in the 2nd dimension as previously described (15). Briefly, primary IEC were resuspended in

lysis buffer containing 7 mol/L urea, 2 mol/L thiourea, 2% 3-[(3-Cholamidopropyl)dimethyl-ammonio]-1-propane sulfonate 1% dithiothreitol, protease inhibitor (Roche Diagnostics), and 2% Pharmalyte (Amersham Biosciences) and homogenized by ultrasonication. For IEF, 500 μg of solubilized total protein was cup-loaded onto rehydrated immobilized pH gradient strips (IPG, pH 3-10, 18 cm, Amersham Biosciences). Subsequent to the first dimension, IPG stripes were loaded onto 12.5% SDS-polyacrylamide gels and gel electrophoresis was performed. After fixation, proteins were stained using a Coomassie Brilliant Blue solution. All 10 gels from RLF mice ($n = 5$) and *L. reuteri* 100-23-colonized RLF mice ($n = 5$) of 1 time point were simultaneously submitted to all steps of 2-dimensional (2D)-gel electrophoresis including IEF, SDS-PAGE, Coomassie Brilliant Blue staining, and quantitative analysis to minimize variability between samples. Coomassie-stained gels were scanned (ImageScanner, Amersham Biosciences) and analyzed by ProteomWeaver software (Definiens), including background subtraction and volume normalization. For each time point, gels from control RLF mice and *L. reuteri* 100-23-colonized RLF mice were compared. Spots picked for further matrix-assisted laser desorption/ionization time of flight (MALDI-TOF) MS analysis differed in protein intensity according to the Mann-Whitney-test ($P < 0.05$) that was at least 1.8-fold of the control group and were present in at least 7 of 10 gels.

Trypsin digestion of protein spots and MALDI-TOF-MS. Coomassie-stained spots were picked, washed, dried, and digested using sequencing grade modified trypsin (Promega) as previously described (15).

We performed mass analysis according to the method of Bruker Daltonics using the Autoflex Control software and the mass spectrometer of Bruker Daltonics. Briefly, 2-3 μL of the extracted protein sample together with 2 μL of 0.1% Trifluoroacetic acid was spotted onto the target using the thin-layer affinity HCCA AnchorChip preparation by Bruker Daltonics. Proteins were identified by using the Mascot Server 1.9 (Bruker Daltonics) based on mass searches within murine sequences only. The search parameters allowed the carboxyamidomethylation of cystein and 1 missing cleavage. We selected the minimum score of 61 and a mass accuracy of $\pm$100 ppm as criteria for positive identification of proteins.

Statistical analysis. All statistical computations were performed using SigmaStat software from Systat Software. Data comparing treatment vs. corresponding control group (in vivo and cell culture experiments) were analyzed using unpaired *t* tests. Time-dependent effects were analyzed using 1-way ANOVA followed by Tukey's test. Histopathology scores are expressed as means $\pm$ SD of 5 different mice per group. Real-time PCR data are expressed as mean fold of control group $\pm$ SD, $n = 5$, measured in duplicates, for the in vivo experiments and as mean fold of control group $\pm$ SD of 2 independent triplicates for the cell culture experiments. Differences between groups were considered significant if *P*-values were < 0.05.

Results

L. reuteri 100-23 induced transient histological changes in the small intestine of RLF mice. Histological analysis of *L. reuteri* 100-23-inoculated RLF mice revealed a slight but significant increase of the histological score associated with increased leukocyte infiltration at d 6 after inoculation (**Fig. 1***A*). However, the histological score remained well below any indication of histopathology. In contrast, no significant differences from the control groups were found 2 and 21 d after inoculation. Population levels of *L. reuteri* increased in the jejunum as well as in the ileum, reaching maximum population levels at d 6 after inoculation (**Table 1**). The transient character of tissue activation emphasizes the nonpathogenicity of *L. reuteri* 100-23, which is present in the normal microbiota of mice (16).

To further test the effects of *L. reuteri* 100-23 on the intestinal epithelium, we isolated total mRNA and protein from primary IEC from the small intestine (ileum and jejunum, pooled) of control and *L. reuteri* 100-23-colonized RLF mice. The cell purity was assessed by determining the absence of $CD3^+$ T cell, $CD19^+$ B cell, and Integrin αX^+ macrophage contaminations (Fig. 1*B*).

L. reuteri 100-23 induced transient changes in gene expression profiles of IEC. For the histological data, we chose to analyze the host transcriptional responses caused by

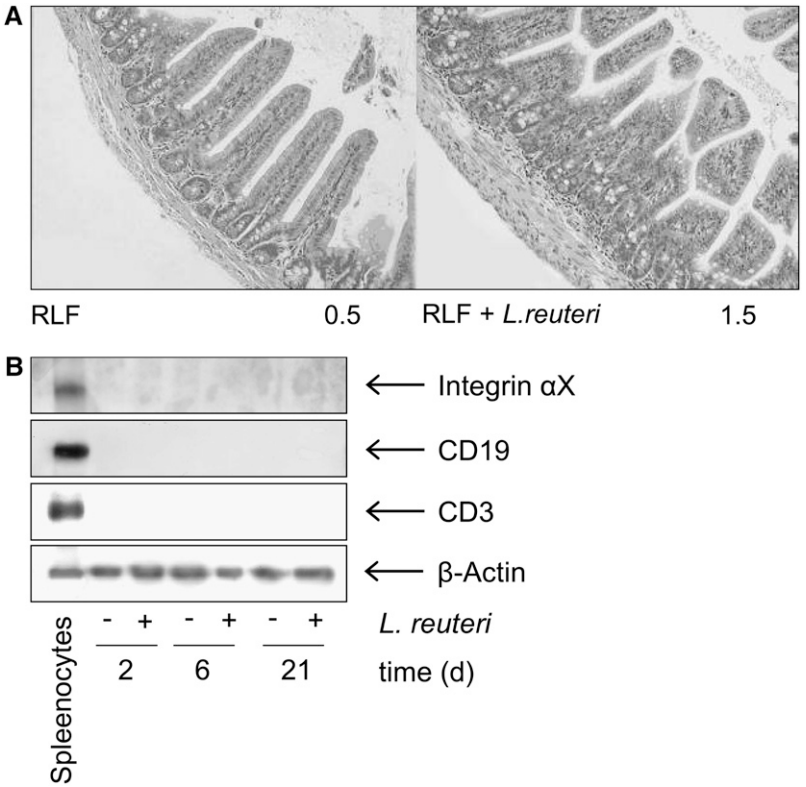

FIGURE 1 Transient histological changes in the small intestine of RLF mice after inoculation with *L. reuteri* 100-23. (*A*) H&E staining of paraffin-embedded tissue sections from a control RLF mouse (left picture) vs. a RLF mouse 6 d after inoculation with *L. reuteri* 100-23 (right picture). The numbers indicate the histological score (0-12) of the specific section. (*B*) Purity of IEC isolates was determined by western blot analysis performed with total protein from primary IEC ($n = 5$, pooled) and splenocytes as positive control using specific antibodies for CD3, CD19, integrin αX, and β-actin.

TABLE 1 Histological score and *L. reuteri* counts in the small intestine from *L. reuteri* 100-23-colonized and control RLF mice

	Histological score[1]	*L. reuteri* count[2]	
Time postinoculation	Ileum	Jejunum	Ileum
d		*CFU log 10/g*	
2			
RLF mice	0.5 ± 0.0	–	–
RLF mice + *L. reuteri*	0.7 ± 0.24[a,b]	3.9	5.4
6			
RLF mice	0.6 ± 0.22	–	–
RLF mice + *L. reuteri*	1.1 ± 0.22*[a]	6.5	7.8
21			
RLF mice	0.40 ± 0.14	–	–
RLF mice + *L. reuteri*	0.55 ± 0.27[b]	6.7	7.9

[1] Values are means ± SD, $n = 5$ (histological score) or 1 (*L. reuteri* count). *Different from RLF mice, *t*-test, $P < 0.05$. Within a group, means with superscripts without a common letter differ over time, ANOVA followed by Tukey-test, $P < 0.05$.
[2] CFU, Colony-forming units.

L. reuteri 100-23 at d 6 after inoculation using Affymetrix NuGO_Mm1a520177 GeneChips for expression analysis. The expression levels of 134 genes were significantly regulated (**Supplemental Table 3**). On the basis of literature cocitation from NCBI PubMed, a bibliometric analysis was performed. The data-mining program Bibliosphere software was used to generate a gene-gene network tree (Bibliosphere Pathway View) (**Supplemental Fig. 1**). Applying a MeSH filter for Gram-positive bacterial infections on the regulated genes results in a network tree comprising interleukin (IL)-1α, IL-6, Cxcl10 [interferon-γ-inducible protein 10 (IP-10)], Cxcl2 [macrophage inflammatory protein 2 (MIP-2)], and Pdia3 (grp-58) (**Fig. 2**; colored version **Supplemental Fig. 2**).

The changes in gene expression at d 6 of these 5 genes and Toll-interacting protein (TOLLIP) were validated using real-time PCR. Additionally, the gene expression levels at d 2 and 21 after *L. reuteri* 100-23 inoculation were determined together with the ability of *L. reuteri* 100-23 to induce these genes in the murine IEC line Mode-K. Furthermore, the mRNA fold changes of control of A20, which negatively regulates nuclear factor (NF)-κB-dependent signaling through tumor necrosis factor, IL-1, and Toll-like receptors (TLR) (17), was determined in primary IEC and Mode-K cells (**Table 2**). The Affymetrix NuGO_Mm1a520177 GeneChip does not contain an appropriate probe set for A20 and therefore A20 was not detectable in the microarray analysis. For all genes examined, real-time PCR data were in good agreement with the gene array results with respect to the direction of observed changes.

Of note, only at d 6 after inoculation with *L. reuteri* 100-23 were significant differences between colonized and control RLF mice detected. Interestingly, the proinflammatory cytokines and chemokines IL-1α, IL-6, IP-10, and MIP-2 had elevated mRNA levels, whereas the mRNA levels of the negative regulators of TLR signaling TOLLIP and A20 (18) and the endoplasmic reticulum (ER) chaperone grp-58 were decreased. In vitro, *L. reuteri* 100-23 significantly induced IL-1α, IL-6, IP-10, and MIP-2.

L. reuteri 100-23 induced transient changes in steady-state protein expression in primary IEC. To further characterize IEC activation in RLF mice following inoculation with *L. reuteri* 100-23, we performed 2D-gel electrophoresis and MALDI-TOF-MS analysis. The mean number of Coomassie-stained protein spots that could be resolved on the 2D SDS-PAGE gels ranged between 600 and 800 spots. Two and 6 d after bacterial inoculation, significantly regulated proteins were present, whereas no regulated protein spots were detected at 21 d after inoculation with *L. reuteri* 100-23. Protein spots regulated 6 d after inoculation are indicated in representative 2D-gels of a control RLF mouse and a *L .reuteri* 100-23-colonized RLF mouse (**Fig. 3***A*). The numbers marking regulated protein spots in the magnified small cut-outs correspond to the numbers in **Table 3**, which compiles all regulated proteins. Interestingly, the only regulated protein spot that could be identified 2 d after inoculation with *L. reuteri* 100-23 was the ER chaperone grp-58 that was also regulated at d 6 after inoculation.

To confirm selected results from the 2D-gel electrophoresis and MALDI-TOF-MS analysis, we performed Western blot analysis using specific antibodies for grp-58 and I-FABP (Fig. 3*B*). For all 3 time points, the number of regulated protein spots and identified proteins are given (Fig. 3*C*).

Discussion

The colonization of RLF mice with nonpathogenic *L. reuteri* 100-23 caused transient leukocyte infiltration in the small intestine 6 d after inoculation, the time point when *L. reuteri* reached stable population levels. The leukocyte infiltration resulted in a significant, but not pathological (<2), increase in the histological score. Most important for the understanding of bacteria-host interaction, the histological changes were reflected by changes in gene and protein expression levels of IEC. Consistently, previous studies in humans showed increased duodenal B-lymphocyte infiltration and higher amounts of CD4-positive T-lymphocytes in the ileal mucosa after dietary supplementation with *L. reuteri*

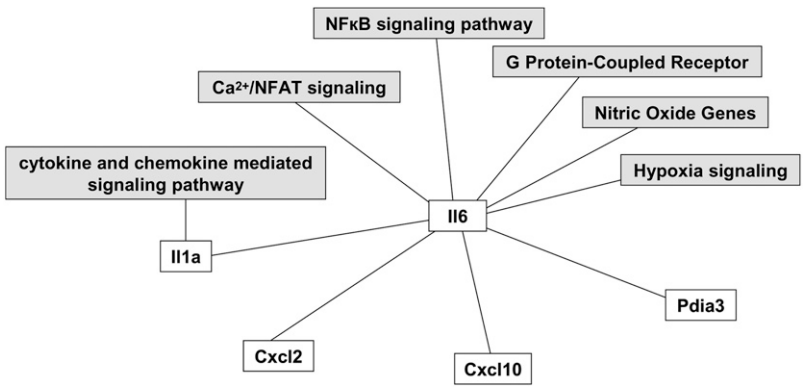

FIGURE 2 Gene-gene network tree based on Affymetrix microarrays and bibliometric analysis. Network tree generated by Biblioshere software after applying a MeSH filter for Gram-positive bacterial infections on the regulated genes, including associated physiological pathways.

TABLE 2 Changes of mRNA levels (fold of control) after inoculation of RLF mice with *L. reuteri* 100-23 or after infection of Mode-K cells with *L. reuteri* 100-23 (multiplicity of infection 30) for various time points, respectively

	Primary IEC,[1] *d*			Mode-K, *h*		
	2	6	21	6	12	24
Cytokines						
IL-1α	3.94 ± 2.57^{a,b}	36.20 ± 6.25$^{\#\#a}$	1.36 ± 0.85^{b}	15.70 ± 2.12$^{\#\#a}$	23.16 ± 4.34$^{\#\#b}$	34.42 ± 2.05$^{\#\#c}$
IL-6	2.49 ± 1.92^{a}	25.21 ± 4.64$^{\#\#b}$	1.89 ± 1.66^{a}	4.88 ± 0.15$^{\#a}$	17.44 ± 2.24$^{\#b}$	5.55 ± 0.43$^{\#a}$
Chemokines						
IP-10	0.77 ± 0.65^{a}	7.98 ± 4,83$^{\#\#b}$	2.55 ± 1.98^{a,b}	2.81 ± 0.58^{a}	10.18 ± 0.97$^{\#b}$	3.33 ± 1.37^{a}
MIP-2	8.88 ± 5.03^{a}	6.59 ± 3.55$^{\#\#a,b}$	1.64 ± 0.71^{b}	29.05 ± 1.01$^{\#\#a}$	18.63 ± 2.67$^{\#\#b}$	12.21 ± 4.45$^{\#c}$
Regulatory						
A20	1.67 ± 2.00^{a,b}	0.15 ± 0.12$^{\#a}$	4.27 ± 3.52^{b}	2.43 ± 0.33$^{\#a}$	0.86 ± 0.14^{b}	0.72 ± 0.02^{a}
TOLLIP	0.13 ± 0.13^{a}	0.19 ± 0.04$^{\#a,b}$	1.02 ± 1.15^{b}	2.20 ± 0.22^{a}	0.58 ± 0.10^{b}	1.44 ± 0.22^{c}
Cell stress						
grp-58	2.32 ± 1.75	0.58 ± 0.19$^{\#}$	1.29 ± 0.96	2.19 ± 0.99	0.43 ± 0.23	2.01 ± 0.79

[1] Values are means ± SD, $n = 5$ (primary IEC) or 2 (Mode-K). Symbols indicate different from the control: *t*-test, $^{\#}P < 0.05$, $^{\#\#}P < 0.001$. For each gene, means with superscripts without a common letter differ over time, ANOVA followed by Tukey-test, $P < 0.05$.

ATCC 55730 (19), confirming the physiological relevance of our findings.

The adaptation of the intestinal mucosa to the presence of commensal bacteria has been studied using germ-free animals associated with single bacterial species or simple mixtures of microorganisms. Kasper et al. (20) showed that monoassociation of germ-free mice with *Bacteroides fragilis* or administration of purified *B. fragilis* surface polysaccharide was sufficient to induce immune maturation in splenic CD4$^+$ T-cell numbers and splenic organization. But it is unknown if and to what extent the intestinal epithelium stays reactive when challenged with non-pathogenic bacteria after the extensive adaptations caused by the

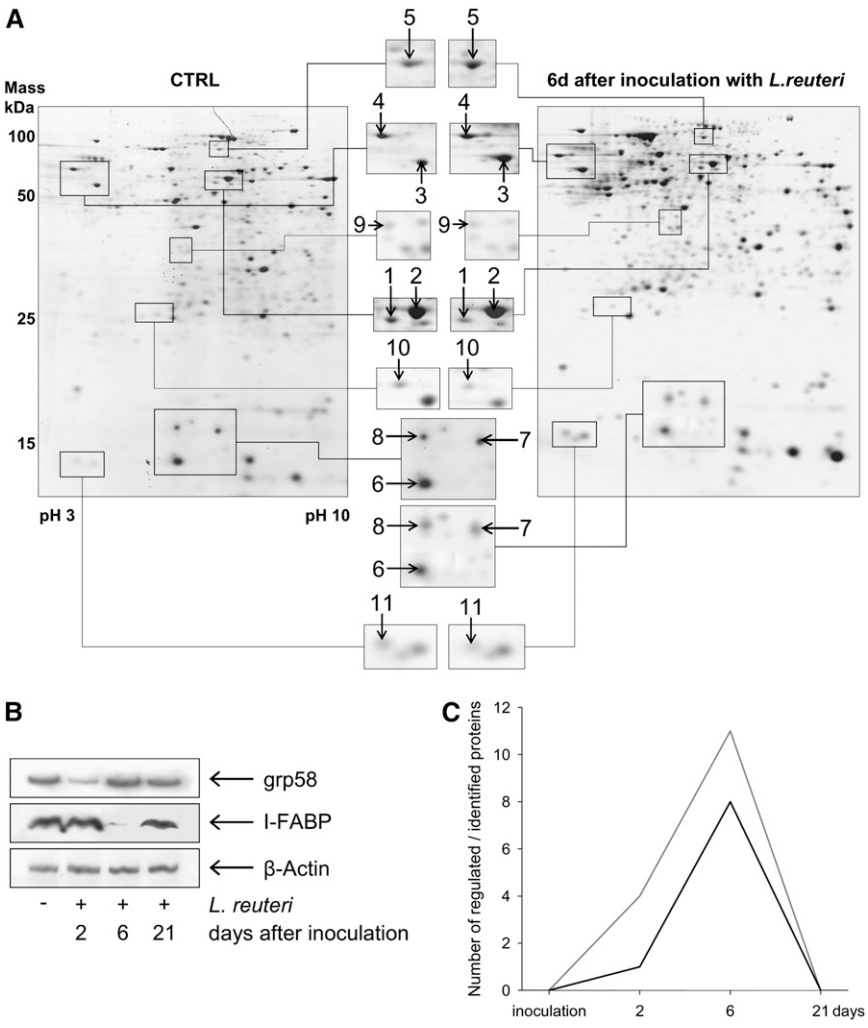

FIGURE 3 Proteome analysis of primary IEC from *L. reuteri* 100-23-colonized RLF mice. (*A*) Regulated protein spots 6 d after inoculation are indicated in representative 2D-gels (big gels) from control and *L. reuteri* 100-23-colonized RLF mice. The numbers indicating regulated protein spots in the magnified small cut-outs correspond to the protein numbers (Table 3). (*B*) Validation of grp-58 and I-FABP protein expression changes in primary IEC after inoculation with *L. reuteri* via western blot analysis. (*C*) Total number of regulated (gray line) and identified (black line) protein spots in primary IEC from the small intestine of RLF mice after inoculation with *L. reuteri* 100-23.

TABLE 3 Differentially regulated proteins identified via 2D-gel electrophoresis and MALDI-TOF MS in IEC from the small intestine of RLF mice 6 d after inoculation with *L. reuteri* 100-23

No.	Protein	Fold of control	U-test	Synonym/description	Function	Subcellular location
1	Aldehyde dehydrogenase family 3, member A2	4.02	0.0159	Fatty aldehyde dehydrogenase Aldh3a2	Aldehyde dehydrogenase (NAD) activity, oxidoreductase activity	Cytoplasmatic surface of the ER membrane
2	Aldehyde dehydrogenase 1 family, member B1	2.33	0.0159	Aldh1b1	Aldehyde dehydrogenase (NAD) activity, carbohydrate metabolism, oxidoreductase activity	Mitochondrion
3	Atp5b protein	6.50	0.0001	ATP synthase, mitochondrial F1 complex, β polypeptide	ATP synthesis coupled proton transport, ATP-binding and phosphorylation-dependent chloride channel activity	Integral to mitochondrial inner membrane
4	Protein disulfide isomerase A3	3.54	0.0001	ERp61, ERp57, Protein disulfide isomerase A3	Electron transporter activity, protein disulfide isomerase activity, chaperone	ER lumen
		0.261[1]	0.0001[1]			
5	Sdha protein	2.70	0.0317	Succinate dehydrogenase complex, subunit A, flavoprotein	Tricarboxylic acid cycle, FAD binding, disulfide oxidoreductase activity	Mitochondrial inner membrane
6	I-FABP	0.55	0.0001	I-FABP	Lipid binding, transporter activity, helps maintain energy homeostasis by functioning as a lipid sensor	Cytoplasm
7	Cellular retinol-binding protein II	0.40	0.0001	CRBP- II	Retinoid binding and metabolism, lipid binding, transporter activity	Cytoplasm
8	Keratin 20	0.43	0.0001	Krt-20, Cytokeratin 20	Structural constituent of cytoskeleton	
9	Unidentified protein	0.54	0.0159			
10	Unidentified protein	0.43	0.0001			
11	Unidentified protein	0.36	0.0317			

[1] Fold change of control and U-test 2 d after *L. reuteri* 100-23 inoculation.

initial colonization. Thus, RLF mice that lack lactobacilli, yet are colonized by a complex microbiota (9), are a promising model to determine the impact of a single bacteria strain/species on the host in a more naturalistic situation.

In several gnotobiotic and germ-free animal models, it has been shown that proinflammatory cytokines were upregulated in response to nonpathogenic bacteria in the intestine (21,22). Notably, also probiotic bacteria strains, e.g. *Bifidobacterium lactis* BB12 and *Lactobacillus fermentum*, induced proinflammatory cytokines such as IP-10, IL-6, or IL-1 in gnotobiotic animal models (21,22).

In our study, RLF mice were inoculated with *L. reuteri*, a Gram-positive bacteria strain that prevented spontaneous and chemically induced colitis in different animal models of chronic inflammation (23-25). *L. reuteri* 100-23 colonizes the gut of formerly lactobacillus-free mice (10,12) and forms a biofilm in the murine forestomach (26). Shedding into the lumen and passing through the remainders of the gastrointestinal tract together with the digesta, lactobacilli can potentially cause activation of IEC in both the small and large intestine of mice. It is attractive to focus on IEC, because the epithelial surface with its mucus layer is the barrier where adaptation to commensal bacteria occurs, because they do not translocate under normal conditions.

In response to *L. reuteri* 100-23, we found transiently increased mRNA levels of the proinflammatory cytokines and chemokines IL-1α, IL-6, IP-10, and MIP-2 in IEC from RLF mice despite the presence of an established microbiota. Using 2D-SDS PAGE and MALDI-TOF MS, we also identified regulated proteins 2 and 6 d after *L. reuteri* inoculation. Not recovering the induction of IL-1α, IL-6, IP-10, and MIP-2 on protein level in this approach is most likely due to the fact that these proteins are secreted and intracellular amounts are beyond the detection limit of Coomassie staining. The regulated proteins found were mainly associated with energy metabolism and did not point to pathological changes but rather toward adaptive mechanisms. Two of these proteins, I-FABP and grp-58, are of particular interest. I-FABP belongs to the fatty acid-binding protein family and adjacent to their function as cytosolic fatty acid chaperones, there is accumulating evidence that FABP integrate metabolic and inflammatory pathways. Macrophages lacking the FABP aP2 show enhanced PPARγ activity and impaired proinflammatory IKK-NF-κB signaling (27). Grp-58 is a disulfide isomerase that belongs to the ER chaperone family. These proteins are upregulated in response to ER stress and have been shown to attenuate cellular death induced by increased intracellular calcium and the accumulation of misfolded proteins in the ER (28). Induction of ER stress responses trigger cell survival mechanisms, whereas prolonged or enhanced ER stress leads to apoptosis (29). In inflamed tissue from IBD patients and in primary IEC from inflamed IL-10−/− mice, activated ER stress responses can be found (15). This suggests that in the absence of adequate control mechanisms, ER stress may contribute to the pathogenesis of IBD (3). Consistent with the absence of pathological changes, grp-58 protein expression returned to control levels in RLF mice 21 d after inoculation.

Despite early inflammatory events, RLF mice do not develop inflammation after *L. reuteri* 100-23 inoculation. By d 21, no differences between control and *L. reuteri*-colonized RLF mice for histological score or gene and protein expression levels were detectable. This points to immunosuppressive mechanisms that control the release of proinflammatory mediators to avoid ongoing leukocyte infiltration and tissue damage after the initial signal that directs immune cells to the site of infection. It has been shown that adjacent lymphocytes regulate IEC activation upon bacterial stimulation (30,31). Also, several TLR pathway intrinsic mechanisms have been proposed for the development of hyporesponsiveness of the intestinal epithelium toward bacterial signals (32-34). *L. reuteri* 100-23, as a Gram-positive bacterium, and its components, such as peptidoglycan, are ligands for TLR2 and are thereby able to initiate signal transduction. It was previously shown that the Gram-positive *B. lactis* BB12 triggered NF-κB and mitogen-activated protein kinase signaling through TLR2 to induce IL-6 expression in IEC (22). Various mechanisms contribute to control TLR activation in IEC, including TOLLIP and A20 (18), 2 negative regulators that exhibit decreased mRNA levels 6 d after *L. reuteri* 100-23 inoculation (17,35). TOLLIP has been implicated in controlling the magnitude of inflammatory cytokine production in response to IL-1β and lipopolysaccharide (36). The expression of A20 is induced by different inflammatory stimuli, including IL-1, and it was shown to inhibit IL-1-induced NF-κB activation (37). A20 gene-deficient mice display multiple spontaneous inflammatory disorders, including colitis, which still develops in $A20^{-/-} \times RAG^{-/-}$ mice, suggesting that A20 may play a role in the control of innate immunity (34,38,39). Combined, our findings in *L. reuteri*-colonized RLF mice suggest that downregulation of the constitutively expressed TOLLIP and A20 may allow transient activation of IEC and thereby an adequate response to new bacterial stimuli.

Our results indicate that the intestinal epithelium is still reactive toward environmental changes induced by the commensal strain *L. reuteri* 100-23 even though the murine hosts have experienced quantitative and qualitative changes in microbiota composition during early life. As some probiotic properties of *L. reuteri* (decreased short-term illnesses) have been observed for up to 80 d (40), it is unlikely that these long-term effects are mediated by IEC. However, the induction of transient IEC activation may help to maintain mucosal homeostasis. Further investigation of the pathways involved in the regulation of innate and/or adaptive immunity and the mechanisms ensuring hyporesponsiveness to the indigenous microbiota may add significant insights into disease pathologies like IBD, where inflammatory processes are due to uncontrolled activation of mucosal cells (3,41). A better understanding of nonpathogenic bacteria signaling in the intestine would help to design new ways to intervene in dysregulated host responses toward normal microbiota.

Literature Cited

1. Rakoff-Nahoum S, Paglino J, Eslami-Varzaneh F, Edberg S, Medzhitov R. Recognition of commensal microflora by toll-like receptors is required for intestinal homeostasis. Cell. 2004;118:229–41.
2. Sartor RB. The influence of normal microbial flora on the development of chronic mucosal inflammation. Res Immunol. 1997;148:567–76.
3. Clavel T, Haller D. Bacteria- and host-derived mechanisms to control intestinal epithelial cell homeostasis: implications for chronic inflammation. Inflamm Bowel Dis. 2007;13:1153–64.
4. Kelly D, Conway S. Bacterial modulation of mucosal innate immunity. Mol Immunol. 2005;42:895–901.
5. Neutra MR, Mantis NJ, Kraehenbuhl JP. Collaboration of epithelial cells with organized mucosal lymphoid tissues. Nat Immunol. 2001; 2:1004–9.
6. Cebra JJ. Influences of microbiota on intestinal immune system development. Am J Clin Nutr. 1999;69:S1046–51.
7. Shroff KE, Meslin K, Cebra JJ. Commensal enteric bacteria engender a self-limiting humoral mucosal immune response while permanently colonizing the gut. Infect Immun. 1995;63:3904–13.
8. Falk PG, Hooper LV, Midtvedt T, Gordon JI. Creating and maintaining the gastrointestinal ecosystem: what we know and need to know from gnotobiology. Microbiol Mol Biol Rev. 1998;62:1157–70.
9. Tannock GW, Crichton C, Welling GW, Koopman JP, Midtvedt T. Reconstitution of the gastrointestinal microflora of lactobacillus-free mice. Appl Environ Microbiol. 1988;54:2971–5.
10. McConnell MA, Mercer AA, Tannock GW. Transfer of plasmid pAM?1 between members of the normal microflora inhabiting the murine digestive tract and modification of the plasmid in a Lactobacillus reuteri host. Microb Ecol Health Dis. 1991;4:343–55.
11. Walter J, Chagnaud P, Tannock GW, Loach DM, Dal Bello F, Jenkinson HF, Hammes WP, Hertel C. A high-molecular-mass surface protein (Lsp) and methionine sulfoxide reductase B (MsrB) contribute to the ecological performance of Lactobacillus reuteri in the murine gut. Appl Environ Microbiol. 2005;71:979–86.
12. Tannock GW. A special fondness for lactobacilli. Appl Environ Microbiol. 2004;70:3189–94.
13. Katakura K, Lee J, Rachmilewitz D, Li G, Eckmann L, Raz E. Toll-like receptor 9-induced type I IFN protects mice from experimental colitis. J Clin Invest. 2005;115:695–702.
14. Ruiz PA, Shkoda A, Kim SC, Sartor RB, Haller D. IL-10 gene-deficient mice lack TGF-beta/Smad signaling and fail to inhibit proinflammatory gene expression in intestinal epithelial cells after the colonization with colitogenic Enterococcus faecalis. J Immunol. 2005;174:2990–9.
15. Shkoda A, Ruiz PA, Daniel H, Kim SC, Rogler G, Sartor RB, Haller D. Interleukin-10 blocked endoplasmic reticulum stress in intestinal epithelial cells: impact on chronic inflammation. Gastroenterology. 2007; 132:190–207.
16. Wesney E, Tannock GW. Association of rat, pig and fowl biotypes of lactobacilli with the stomach of gnotobiotic mice. Microb Ecol. 1979;5:35–42.
17. Gon Y, Asai Y, Hashimoto S, Mizumura K, Jibiki I, Machino T, Ra C, Horie T. A20 inhibits toll-like receptor 2- and 4-mediated interleukin-8 synthesis in airway epithelial cells. Am J Respir Cell Mol Biol. 2004; 31:330–6.
18. Shibolet O, Podolsky DK. TLRs in the gut. IV. Negative regulation of Toll-like receptors and intestinal homeostasis: addition by subtraction. Am J Physiol Gastrointest Liver Physiol. 2007;292:G1469–73.
19. Valeur N, Engel P, Carbajal N, Connolly E, Ladefoged K. Colonization and immunomodulation by Lactobacillus reuteri ATCC 55730 in the human gastrointestinal tract. Appl Environ Microbiol. 2004;70:1176–81.
20. Mazmanian SK, Liu CH, Tzianabos AO, Kasper DL. An immunomodulatory molecule of symbiotic bacteria directs maturation of the host immune system. Cell. 2005;122:107–18.
21. Shirkey TW, Siggers RH, Goldade BG, Marshall JK, Drew MD, Laarveld B, Van Kessel AG. Effects of commensal bacteria on intestinal morphology and expression of proinflammatory cytokines in the gnotobiotic pig. Exp Biol Med (Maywood). 2006;231:1333–45.
22. Ruiz PA, Hoffmann M, Szcesny S, Blaut M, Haller D. Innate mechanisms for Bifidobacterium lactis to activate transient pro-inflammatory host responses in intestinal epithelial cells after the colonization of germ-free rats. Immunology. 2005;115:441–50.
23. Fabia R, Ar'Rajab A, Johansson ML, Willen R, Andersson R, Molin G, Bengmark S. The effect of exogenous administration of Lactobacillus reuteri R2LC and oat fiber on acetic acid-induced colitis in the rat. Scand J Gastroenterol. 1993;28:155–62.
24. Mao Y, Nobaek S, Kasravi B, Adawi D, Stenram U, Molin G, Jeppsson B. The effects of Lactobacillus strains and oat fiber on methotrexate-induced enterocolitis in rats. Gastroenterology. 1996;111:334–44.
25. Madsen KL, Doyle JS, Jewell LD, Tavernini MM, Fedorak RN. Lactobacillus species prevents colitis in interleukin 10 gene-deficient mice. Gastroenterology. 1999;116:1107–14.
26. Tannock GW, Ghazally S, Walter J, Loach D, Brooks H, Cook G, Surette M, Simmers C, Bremer P, et al. Ecological behavior of Lactobacillus reuteri 100-23 is affected by mutation of the luxS gene. Appl Environ Microbiol. 2005;71:8419–25.

27. Makowski L, Brittingham KC, Reynolds JM, Suttles J, Hotamisligil GS. The fatty acid-binding protein, aP2, coordinates macrophage cholesterol trafficking and inflammatory activity. Macrophage expression of aP2 impacts peroxisome proliferator-activated receptor gamma and IkappaB kinase activities. J Biol Chem. 2005;280:12888–95.
28. Mazzarella RA, Marcus N, Haugejorden SM, Balcarek JM, Baldassare JJ, Roy B, Li LJ, Lee AS, Green M. Erp61 is GRP58, a stress-inducible luminal endoplasmic reticulum protein, but is devoid of phosphatidylinositide-specific phospholipase C activity. Arch Biochem Biophys. 1994;308:454–60.
29. Kadowaki H, Nishitoh H, Ichijo H. Survival and apoptosis signals in ER stress: the role of protein kinases. J Chem Neuroanat. 2004;28:93–100.
30. Haller D, Holt L, Kim SC, Schwabe RF, Sartor RB, Jobin C. Transforming growth factor-beta 1 inhibits non-pathogenic Gram negative bacteria-induced NF-kappa B recruitment to the interleukin-6 gene promoter in intestinal epithelial cells through modulation of histone acetylation. J Biol Chem. 2003;278:23851–60.
31. Haller D, Russo MP, Sartor RB, Jobin C. IKK beta and phosphatidylinositol 3-kinase/Akt participate in non-pathogenic Gram-negative enteric bacteria-induced RelA phosphorylation and NF-kappa B activation in both primary and intestinal epithelial cell lines. J Biol Chem. 2002;277:38168–78.
32. Lotz M, Gutle D, Walther S, Menard S, Bogdan C, Hornef MW. Postnatal acquisition of endotoxin tolerance in intestinal epithelial cells. J Exp Med. 2006;203:973–84.
33. Zhang G, Ghosh S. Negative regulation of toll-like receptor-mediated signaling by Tollip. J Biol Chem. 2002;277:7059–65.
34. Boone DL, Turer EE, Lee EG, Ahmad RC, Wheeler MT, Tsui C, Hurley P, Chien M, Chai S, et al. The ubiquitin-modifying enzyme A20 is required for termination of Toll-like receptor responses. Nat Immunol. 2004;5:1052–60.
35. Janssens S, Beyaert R. Role of Toll-like receptors in pathogen recognition. Clin Microbiol Rev. 2003;16:637–46.
36. Didierlaurent A, Brissoni B, Velin D, Aebi N, Tardivel A, Kaslin E, Sirard JC, Angelov G, Tschopp J, Burns K. Tollip regulates proinflammatory responses to interleukin-1 and lipopolysaccharide. Mol Cell Biol. 2006;26:735–42.
37. Heyninck K, Beyaert R. The cytokine-inducible zinc finger protein A20 inhibits IL-1-induced NF-kappaB activation at the level of TRAF6. FEBS Lett. 1999;442:147–50.
38. Dumitru CD, Ceci JD, Tsatsanis C, Kontoyiannis D, Stamatakis K, Lin JH, Patriotis C, Jenkins NA, Copeland NG, et al. TNF-alpha induction by LPS is regulated posttranscriptionally via a Tpl2/ERK-dependent pathway. Cell. 2000;103:1071–83.
39. Lee EG, Boone DL, Chai S, Libby SL, Chien M, Lodolce JP, Ma A. Failure to regulate TNF-induced NF-kappaB and cell death responses in A20-deficient mice. Science. 2000;289:2350–4.
40. Tubelius P, Stan V, Zachrisson A. Increasing work-place healthiness with the probiotic Lactobacillus reuteri: a randomised, double-blind placebo-controlled study. Environ Health. 2005;4:25.
41. Haller D. Intestinal epithelial cell signalling and host-derived negative regulators under chronic inflammation: to be or not to be activated determines the balance towards commensal bacteria. Neurogastroenterol Motil. 2006;18:184–99.